J. Biochem. 132, 573–579 (2002)

Formation and Characterization of Kinesin·ADP·Fluorometal Complexes[1]

Hideka Shibuya, Kazunori Kondo, Naohiro Kimura, and Shinsaku Maruta[2]

Department of Bioengineering, Faculty of Engineering, Soka University, Hachioji, Tokyo 192-8577

Received June 21, 2002; accepted July 22, 2002

Recent crystallographic studies of motor proteins showed that the structure of the motor domains of myosin and kinesin are highly conserved. Thus, these motor proteins, which are important for motility, may share a common mechanism for generating energy from ATP hydrolysis. We have previously demonstrated that, in the presence of ADP, myosin forms stable ternary complexes with new phosphate analogues of aluminum fluoride (AlF_4^-) and beryllium fluoride (BeF_n), and these stable complexes mimic the transient state along the ATPase kinetic pathway [Maruta *et al.* (1993) *J. Biol. Chem.* 268, 7093–7100]. In this study, we examined the formation of kinesin·ADP·fluorometals ternary complexes and analyzed their characteristics using the fluorescent ATP analogue NBD-ATP (2′(3′)-*O*-[6-(*N*-(7-nitrobenz-2-oxa-1,3-diazol-4-yl)amino)hexanoyl]-ADP). Our results suggest that these ternary complexes may mimic transient state intermediates in the kinesin ATPase cycle. Thus, the kinesin·ADP·AlF_4^- complex resembles the kinesin·ADP state, and the kinesin·ADP·BeF_n complex mimics the kinesin·ADP·P_i state.

Key words: cell motility, energy-transduction, kinesin.

Kinesin is an ATP-driven motor protein that plays important physiological roles in intracellular transport, mitosis and meiosis, control of microtubule dynamics and signal transduction. Recent structural analyses of kinesin (*1–4*) have shown that it is strikingly similar in structure to the catalytic domains of myosin and G-protein (*5, 6*). This similarity suggests that the motor proteins and molecular switches, which convert energy from ATP into force production for motility and switching, use a similar conformational strategy at the first stage of energy transduction.

However, the motility properties of the microtubule-kinesin system are significantly different from the actomyosin system. Kinesin was found to be a highly processive motor molecule that moves a microtubule in more than 100 consecutive 8-nm steps before dissociating (*7, 8*). In contrast, myosin executes a single stroke and immediately dissociates from actin (*9, 10*). These distinctions suggest that the mechanochemical coupling of kinesin may be somewhat different from that of myosin. Various kinetic studies have demonstrated that the microtubule-kinesin and actomyosin mechanisms appear to follow different pathways. Dissociation of the kinesin occurs after the hydrolysis step, whereas dissociation occurs before hydrolysis for actomyosin (*11*). These kinetic differences may indicate the coupling of a different step to generate force.

For the motor proteins to produce forward motion, the ATPase cycle must be linked to a conformational change in the cycle. However, it is not clear how the two motor proteins change their conformation during the ATPase cycle, a process directly related to energy transduction. Since intermediates in the ATPase cycle are transient, with only a limited lifetime, identification of stable analogues corresponding to these intermediates would be useful. Biochemical studies have demonstrated that in the presence of Mg^{2+}-ADP and certain fluorometals, aluminum fluoride (AlF_4^-) (*12, 13*), beryllium fluoride (BeF_n) (*12–14*), scandium fluoride (ScF_n) (*15*), gallium fluoride (GaF_n) (*16*), and magnesium fluoride (MgF_n) (*17, 18*), myosin forms stable myosin·Mg^{2+}-ADP·fluorometal ternary complexes. Each of these stable complexes mimics specific steps in the ATPase kinetic pathway. Recent crystallographic studies (*19, 20*) have also identified differences between the ternary complexes (AlF_4^-, BeF_n, V_i) in the conformation of the COOH-terminal segment of the truncated myosin head from *Dictyostelium discoideum* myosin II (S-1 Dc). The ternary complexes for G-proteins induced by fluorometals of AlF_4^- and BeF_n also work in a manner similar to myosin to form G-protein·GDP·AlF_4^- or BeF_n ternary complexes that mimic GTPase transient intermediates, resulting in G-protein activation (*21–24*). Therefore, it is of interest to determine whether kinesin also forms ternary complexes with ADP and fluorometals that may mimic the transient intermediates of the kinesin ATPase kinetic pathway in a manner similar to that of myosin and G-proteins.

In the present study, the fluorescent ADP analogue NBD-ADP was employed to monitor the formation of kinesin·ADP·fluorometal ternary complexes. Because the formation of the myosin·ADP·fluorometal ternary complexes

[1]This work was supported by Grants in Aid for Scientific Research C (#11680667) from the Ministry of Education, Science, Sports and Culture of Japan.

[2]To whom correspondence should be addressed. Tel: +81-426-91-9443, Fax: +81-426-91-9312, E-mail: shinsaku@t.soka.ac.jp

Abbreviations: AlF_4^-, aluminum fluoride; BeF_n, beryllium fluoride; DTT, dithiothreitol; GaF_n, gallium fluoride; IPTG, isopropyl-β-D-thiogalactopyranoside; K, kinesin; KHC, kinesin heavy chain; KLC, kinesin light chain; MgF_n, magnesium fluoride; MKH350, kinesin motor domain; MT, microtubule; NBD-ATP, 2′(3′)-*O*-[6-(*N*-(7-nitrobenz-2-oxa-1,3-diazol-4-yl)amino)hexanoyl]-ADP; P_i, phosphate; PNK, polynucleotide kinase; ScF_n, scandium fluoride; V_i, vanadate.

could be monitored successfully by use of the ADP analogue, the stability and interaction of microtubules with the ternary complexes were also examined to determine whether the complexes mimic the transient steps in the microtubule-activated kinesin kinetic pathway.

MATERIALS AND METHODS

Materials—Restriction enzymes and other enzymes were purchased from Toyobo (Tokyo) unless otherwise noted. Oligonucleotides were synthesized by Sawady (Tokyo). The Ni-chelating column was from Sigma (St. Louis, MO). Chemicals were purchased from Wako Pure Chemicals (Osaka) unless otherwise described. ATP, ADP, dithiothreitol (DTT), beryllium sulfate ($BeSO_4$), aluminum chloride ($AlCl_3$), vanadium (V_i), and sodium fluoride (NaF) were purchased from Wako Pure Chemicals. Tubulin was purified from porcine brain as described by Hackney (*25*).

Cloning of the KIF5A Motor Domain cDNA—The 5′-primer of the motor domain was the same as the 5′-primer for the full-length cDNA. A 3′-primer (5′-AGAGGATCCTTAATTCACTGAGGCAGTGTTCT-3′) was used to introduce a stop codon (underlined nucleotide triplet) next to Ala (334) and a *Bam*HI site 5′ to it. The 3,081 bp full-length PCR-amplified fragment was purified by 1% agarose gel and used as a template primer for PCR amplification. PCR was carried out with KOD-plus under the following conditions: 1 cycle at 94°C for 2 min, follow by 35 cycles of 94°C for 30 s, 55°C for 15 s, and 68°C for 3.5 min with QT-II. A single band of 1,002 bp was observed by agarose gel electrophoresis. The 1,002 bp *Bam*HI fragment was cloned into a *Bam*HI site of pBluscript SK⁻ as described above. The 1,002 bp *Bam*HI fragment was then subcloned into a *Bam*HI site of an expression vector pET15b (pET15b::MKH350). The cDNA sequence was confirmed by the dideoxy chain termination method with a SQ-5500 sequencer (Hitachi, Tokyo) using the Genetyx program (Software Development).

Expression of Kinesin—*Escherichia coli* BL21(DE3) strain was transformed with pET21a::MKH350 for large-scale expression of the recombinant kinesin protein. Transformants were selected on L-plates with 100 μg/ml ampicillin. For purification of protein, *E. coli* was grown at 37°C for 18 h in 500 ml of L-broth with 100 μg/ml ampicillin to an absorbance at 600 nm of 1.5, then 0.1 mM of IPTG and 0.1 mM DTT were added, and incubation was continued at 37°C for 3 h. Cells were collected by centrifugation and stored at –80°C until use. The frozen cells were thawed and suspended with 5 ml of sonication buffer with 0.1 mM DTT and sonicated for 15 min at 5 of micro tip limit at 40% of duty cycle in an Ultras Homogenizer VP-30S (Taitec). The sample was clarified by ultra-centrifugation for 45 min, and the supernatant was stored at 4°C until use.

Purification of Recombinant Kinesin Motor Domain—The stored supernatant was loaded on Ni-chelating column which had been equilibrated with native buffer (30 mM Tris-HCl pH 7.8, and 300 mM NaCl). The column was washed with native buffer, then with native buffer containing 50 mM imidazole. The desired protein was eluted with 100 mM imidazole in native buffer, and the fractions containing kinesin were pooled. Purity was assessed by sodium dodecyl sulfate–polyacrylamide gel electrophoresis (SDS-PAGE), which revealed a single band on Coomassie-stained gels. Samples were dialyzed against 120 mM Tris-HCl, 30 mM NaCl, and 1 mM DTT, pH 7.5, and stored at –80°C until use.

ATPase Assays—The ATPase assay was performed for 1 μM MKH in the presence of 2 mM ATP, 50 mM KCl, 50 mM imidazole-HCl, pH 6.7, 3 mM $MgCl_2$, 0.1 mM EDTA, 1 mM EGTA, 1 mM β-mercaptoethanol, and in the presence or absence of 5 μM microtubule.

SDS-PAGE—Protein analysis was performed in 7.5–20% polyacrylamide gradient slab gels in the presence of 0.1% SDS at a constant voltage (200 V) in the discontinuous buffer system of Laemmli (*26*). Peptide bands were visualized by staining with Coomassie Brilliant Blue. Molecular masses of the peptide bands were estimated by comparing their mobility with markers of known molecular weight.

Fluorescence Measurement and Formation of Kinesin·NBD-ADP·Fluorometal Ternary Complexes—Fluorescence was measured at 25°C with a F-2500 spectrofluorometer (Hitachi). The fluorescent ADP analogue, NBD-ADP, was synthesized according to Maruta *et al.* (*27*), with slight modification of the method described by Guillory and Jeng (*28*). The change in fluorescence intensity of 0.3 μM NBD-ADP in the presence of 1.5 μM MKH on addition of nucleotides or P_i analogues (1 mM AlF_4^-, 1 mM BeF_n, or 1 mM V_i) was monitored in a solution of 20 mM NaCl, 30 mM Tris-HCl, pH 7.5, and 2 mM $MgCl_2$. The excitation and emission wavelengths were 475 and 535 nm, respectively.

MT Pelleting Assays—The pelleting assays were performed according to Lockhart *et al.* (*29*). To 4 μM of kinesin motor domain in a buffer of 20 mM MOPS, pH 7.2, were added 1 mM DTT, 5 mM $MgCl_2$, 25 mM NaCl, 1 mM ATP, 1 mM ADP, 1 mM ADP + 1 mM fluorometals or no nucleotide, and the mixture was allowed to stand for 10 min at 25°C. Subsequently 6 μM MTs was added and the solution was gently mixed, then incubated for 10 min at 25°C, and centrifuged at 80,000 rpm for 20 min at 25°C (himac RP100AT3, Hitachi). The supernatants and pellet were run on SDS slab gel and stained with Coomassie Brilliant Blue.

RESULTS

Preparation of Mouse Brain Kinesin Head Domain—The DNA fragments encoding the N-terminal 350 amino acids of mouse brain kinesin head domain (MKH350) were generated by PCR as described in "MATERIALS AND METHODS." The DNA fragment was ligated to the vector pET-15b, which had been digested with *Bam*HI. This chimeric plasmid generates a fusion protein in which the kinesin insert is fused at the N-terminus to a sequence of six histidine residues, which allows for affinity purification by Ni-NTA agarose. As shown in Fig. 1A, MKH350 was eluted as peak C from Ni-NTA agarose columns by addition of 100 mM imidazole. Its separation from the other proteins of *E. coli* was analyzed by SDS-PAGE, which showed that the fractions of peak C contain only highly pure kinesin (Fig. 1B). Amino acid sequence analysis showed that the purified protein has, following the 6-His tag in its N-terminal region, an identical sequence to mouse brain kinesin (1–20 amino acids analyzed).

ATPase in the Presence and Absence of Microtubules—In the absence of MTs, the basal steady-state ATPase activity of MKH350 was very low (2.52 P_i mol/site mol/min). The value was similar to that of bovine brain kinesin (2.40 P_i mol/site mol/min), suggesting that the activity was in the

normal range. The addition of microtubules markedly increased the ATPase activity of MKH350 (114.5 P_i mol/site mol/min), as seen in native kinesins.

Formation of the Kinesin·ADP·Fluorometal Ternary Complexes—We employed the fluorescent ATP analogue, 2′(3′)-*O*-{6-(*N*-(7-nitrobenz-2-oxa-1,3-diazol-4-yl)amino)hexanoyl}-ATP (NBD-ATP), to monitor the ternary complexes of MKH350 with ADP and P_i analogue of fluorometals. As shown in Fig. 2, NBD-ADP carries NBD fluorophore at the 2′ or 3′ position of ribose *via* an aminohexanoic spacer, which is highly environmentally sensitive. Upon addition of 1.5 μM MKH350 to 0.3 μM NBD-ATP, the fluorescence intensity at 535 nm rapidly increased by 3-fold (Fig. 3). Subsequently, the fluorescence decreased slightly due to hydrolysis of NBD-ATP to NBD-ADP and plateaued. However, the fluorescence intensity fell to the level before addition of MKH350 upon addition of 100 μM ATP. These results suggest that enhancement of NBD-ATP fluorescence reflects the binding of NBD-ATP to the ATPase site of MKH350, and distinguishes the states of kinesin·ADP and kinesin·ATP. The rapid initial binding was also analyzed by stopped flow and compared with the results of Mant-ATP reported by Ma and Taylor (*30*). The apparent second-order rate constant for NBD-ATP was 11 $\mu M^{-1} s^{-1}$, similar to that for Mant-ATP (9 $\mu M^{-1} s^{-1}$).

Using NBD-ATP, we then monitored the formation of kinesin·ADP·fluorometal ternary complexes. After the complete hydrolysis of NBD-ATP to NBD-ADP, phosphate analogues were added to start formation of the ternary complexes. Upon addition of 1 mM BeF_n, the fluorescence was reduced by 25% as shown in Fig. 4B. Subsequently, the addition of 60 μM ATP restored the fluorescence to the same level before addition of MKH350, due to the release of NBD-ADP from the ATPase site. These results suggested that the ternary complex is not as stable as myosin·ADP·fluorometals, which are not decomposed by excess ATP (*12*). For V_i, a similar decrease in fluorescence was observed, but the degree of reduction (by 40%) was higher than that of BeF_n (Fig. 4C). Furthermore, the addition of excess ATP almost completely released NBD-ADP from the ATP binding site. Inset of Fig. 4B shows the linearity of the fluorescence change depending on the amount of NBD-ADP bound to MKH350, resulting in formation of MKH350·NBD-ADP·BeF_n ternary complex. In contrast with BeF_n and V_i, upon addition of AlF_4^-, the fluorescence intensity

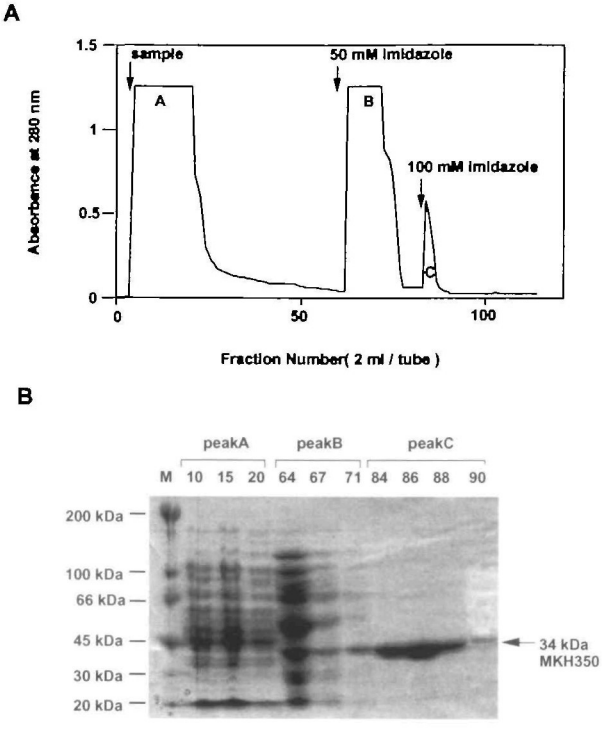

Fig. 1. **Affinity purification of MKH350 protein by Ni-NTA agarose.** (A) After loading the sample, the column was washed for 1 h at 0.8 ml/min with native buffer (30 mM Tris-HCl, pH 7.8, and 300 mM NaCl) and subsequently with 50 mM imidazole-containing native buffer. The desired protein was eluted with 100 mM imidazole in native buffer. Two-milliliter fractions were collected, and ultraviolet-absorbing fractions of peak C were pooled. (B) Purity was assessed by sodium dodecyl sulfate–polyacrylamide gel electrophoresis, which revealed a single band on Coomassie-stained gels.

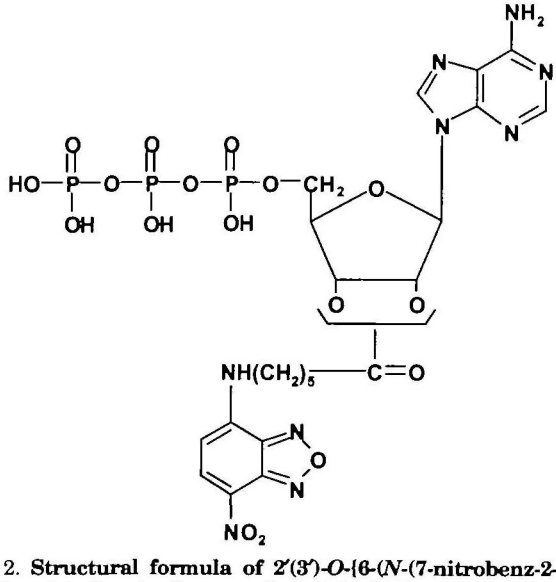

Fig. 2. **Structural formula of 2′(3′)-*O*-{6-(*N*-(7-nitrobenz-2-oxa-1,3-diazol-4-yl)amino)hexanoyl}-ATP (NBD-ATP).**

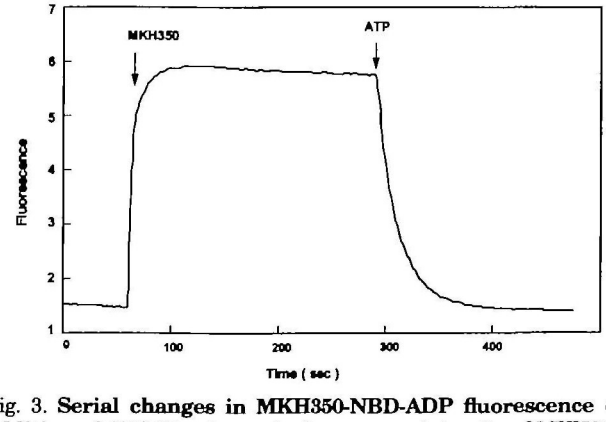

Fig. 3. **Serial changes in MKH350-NBD-ADP fluorescence on addition of ATP.** The change in fluorescence intensity of MKH350-NBD-ADP on addition of nucleotides was monitored in a solution of 120 mM NaCl, 30 mM Tris-HCl, pH 7.5, 2 mM $MgCl_2$ containing 0.3 μM NBD-ATP and 1.5 μM MKH350 at 25°C. The excitation and emission wavelengths were 475 and 535 nm, respectively.

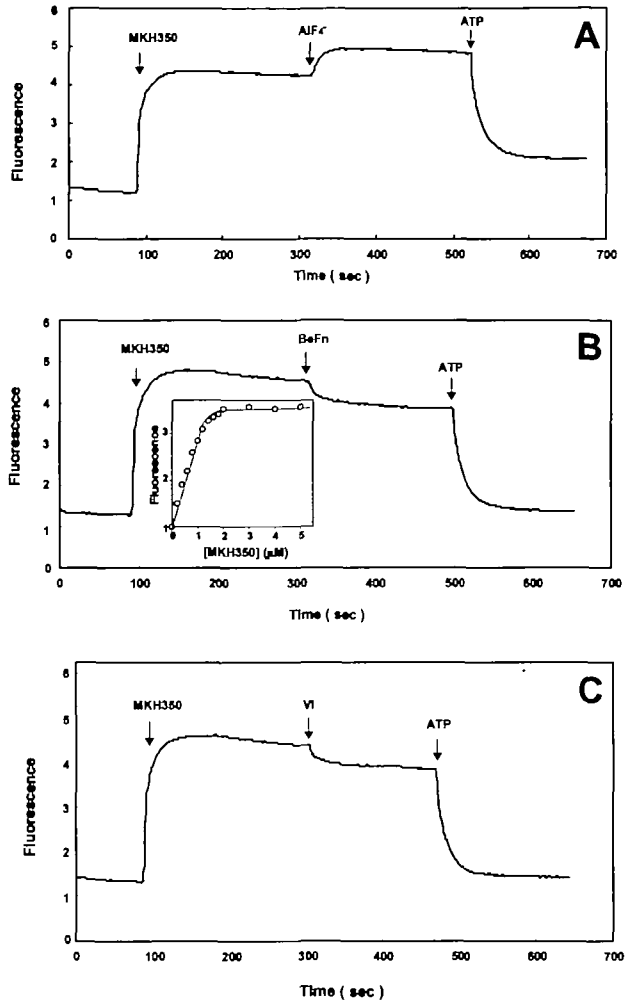

Fig. 4. **Serial changes in NBD-ADP fluorescence on binding to MKH350 and dissociating from MKH350 upon addition of excess ATP.** The change in fluorescence intensity of MKH350·NBD-ADP on addition of nucleotides or P_i analogues (A: AlF_4^-, B: BeF_n, C: V_i) was monitored in a solution of 120 mM NaCl, 30 mM Tris-HCl, pH 7.5, and 2 mM $MgCl_2$ containing 0.3 μM NBD-ATP and 1.5 μM MKH350 at 25°C. The excitation and emission wavelengths were 475 nm and 535 nm, respectively. Inset of Fig. 4B: Fluorescence change depending on the concentration of MKH350 in the presence of BeF_n. To 1 μM NBD-ADP in the solution of 120 mM NaCl, 30 mM Tris-HCl pH 7.5, 2 mM $MgCl_2$, and 1 mM BeF_n, 0–5 μM MKH350 was added at 25°C.

TABLE I. **Rate constants of formation of MKH350·NBD-ADP·fluorometal ternary complexes.** Values of rate constants (k) were determined under the following conditions: 120 mM NaCl, 30 mM Tris-HCl, 2 mM $MgCl_2$, 5 mM DTT, pH 7.5, 25°C for 1.5 μM MKH350 in the presence of 1 mM BeF_n (MKH350·ADP·BeF_4); 1 mM AlF_4^- (MKH350·ADP·AlF_4^-); or 1 mM sodium vanadate (MKH350·ADP·V_i).

Sample	k (s^{-1})		
	ADP·AlF_4^-	ADP·BeF_n	ADP·V_i
Myosin	0.0023	0.07	0.012
MKH350 – MTs	0.12	0.022	0.059
MKH350 + MTs	0.096	0.028	0.034

increased to the same level as that induced by initial binding of NBD-ATP (Fig. 4A). These results suggest that the fluorophore NBD-ADP bound to the ATPase site with AlF_4^- is in a different state from that in the complexes of BeF_n and V_i. Moreover, despite the addition of excess ATP, 25% of the fluorescence enhancement was still seen, indicating the formation of a stable kinesin·ADP·AlF_4^- ternary complex. The rate constants for formation of kinesin·ADP·fluorometal ternary complex, which were estimated from the time course of the fluorescence change, fitted an exponential profile after the addition of fluorometals. The rate constants obtained are summarized in Table I and compared with the rate constants for the formation of myosin·ADP·fluorometal ternary complexes measured under similar conditions. For the BeF_n and V_i complexes, there were no significant differences between the rate constants for kinesin and myosin. We have previously shown that the formation of myosin·ADP·AlF_4^- is very slow (*12*), as shown in Table I. In contrast, the formation of the ternary complex with AlF_4^- is approximately 50-fold faster for kinesin than for myosin.

Release of NBD-ADP from the Ternary Complexes by Chasing with ATP—To confirm the formation of the kinesin·ADP·fluorometal ternary complexes, ATP concentration dependency of ADP release from the ternary complexes was examined. The dissociation of ADP from the complexes was monitored as fluorescence change of NBD-ADP. The time-course of fluorescence decrease fitted an exponential profile, yielding rate constants. Figure 5 is a plot of the rate constants of dissociation of the bound NBD-ADP in the ternary complexes against concentration of ATP. In the absence of fluorometals, ATP released the NBD-ADP at a maximum rate of 0.1 s^{-1}. In the presence of fluorometals, the maximum rates were reduced to 0.07 s^{-1} for BeF_n, 0.06 s^{-1} for V_i, and 0.04 s^{-1} for AlF_4^-, reflecting the formation of kinesin·ADP·fluorometals ternary complexes.

As shown in Fig. 6, microtubules accelerated the release of NBD-ADP, and the maximum rate in the absence of fluo-

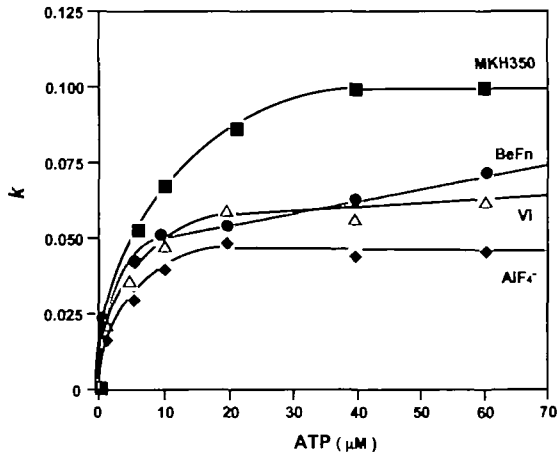

Fig. 5. **Release of NBD-ADP from MKH350·NBD-ADP·fluorometals ternary complexes.** ATP concentration-dependent rate constants of release of NBD-ADP from MKH350·NBD-ADP·P_i analogues ternary complexes were measured by monitoring fluorescence change of NBD-ADP. The k values were determined under the following conditions: 0.3 μM NBD-ATP, 1.5 μM MKH350, 120 mM NaCl, 30 mM Tris-HCl, 2 mM $MgCl_2$, 5 mM DTT, and 1 mM fluorometals, pH 7.5 at 25°C.

rometals was 4-fold greater in the presence of microtubules. Release of NBD-ADP in the presence of fluorometals was also accelerated, but the maximum rate for AlF_4^- was one half of those for BeF_n and V_i.

In Fig. 7, the rates of dissociation of the bound NBD-ADP in the ternary complexes are related to microtubule concentration. The release of NBD-ADP in the presence of BeF_n and V_i was accelerated with increased concentration of microtubules. For the BeF_n complex, the dependence fitted a hyperbola with a maximum rate of 0.5 s^{-1} and the concentration for half-maximum rate of 1.2 μM. Likewise, the release of NBD-ADP in the presence of V_i showed similar values. In contrast, in the presence of AlF_4^-, the release was independent of the concentration of microtubules. These results may suggest that microtubules do not readily bind with MKH350·ADP·AlF_4^- complex. On the other hand, microtubules readily bind to the other complexes, thereby accelerating the release of ADP.

To confirm this, the binding stoichiometries of MKH350·ADP·fluorometals ternary complexes were measured using the microtubule pelleting assay. The contents of MKH350 dissociated from microtubules was estimated from the protein bands in SDS-PAGE shown in Fig. 8A using an image analyzer, and the results are summarized in Fig. 8B. Under

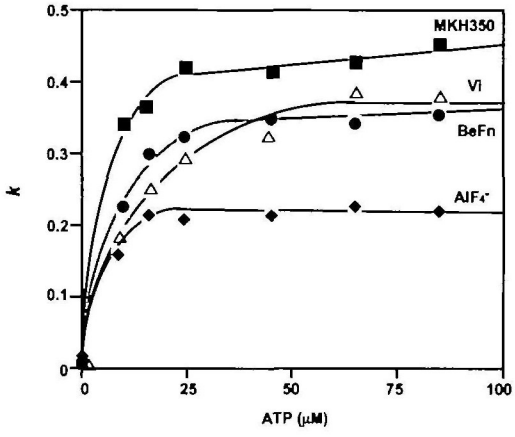

Fig. 6. **Release of NBD-ADP from MKH350-NBD-ADP-fluorometals ternary complexes in the presence of microtubules.** ATP concentration-dependent rate constants (k) of release of NBD-ADP from MKH350-NBD-ADP-P_i analogues ternary complexes were measured by monitoring NBD-ADP fluorescence changes. The k values were determined under the following conditions: 120 mM NaCl, 30 mM Tris-HCl, 2 mM $MgCl_2$, and 5 mM DTT, pH 7.5, 0.3 μM NBD-ATP, 1.5 μM MKH350, 1.5 μM microtubules, and 1 mM fluorometals at 25°C.

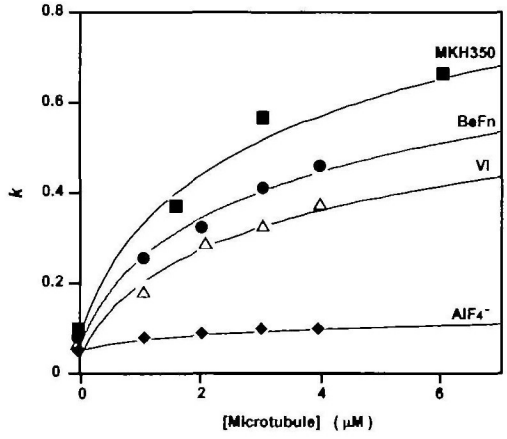

Fig. 7. **Release of NBD-ADP from MKH350-NBD-ADP-fluorometals ternary complexes in the presence of microtubules.** Microtubule concentration-dependent rate constants of release of NBD-ADP from MKH350·NBD·ADP-P_i analogues ternary complexes were measured by monitoring NBD-ADP fluorescence changes. The k values were determined under the following conditions: 120 mM NaCl, 30 mM Tris-HCl, 2 mM $MgCl_2$, and 5 mM DTT, pH 7.5, 25°C for 1.5 μM MKH350, 0.3 μM NBD-ADP, and 0–6 μM microtubules.

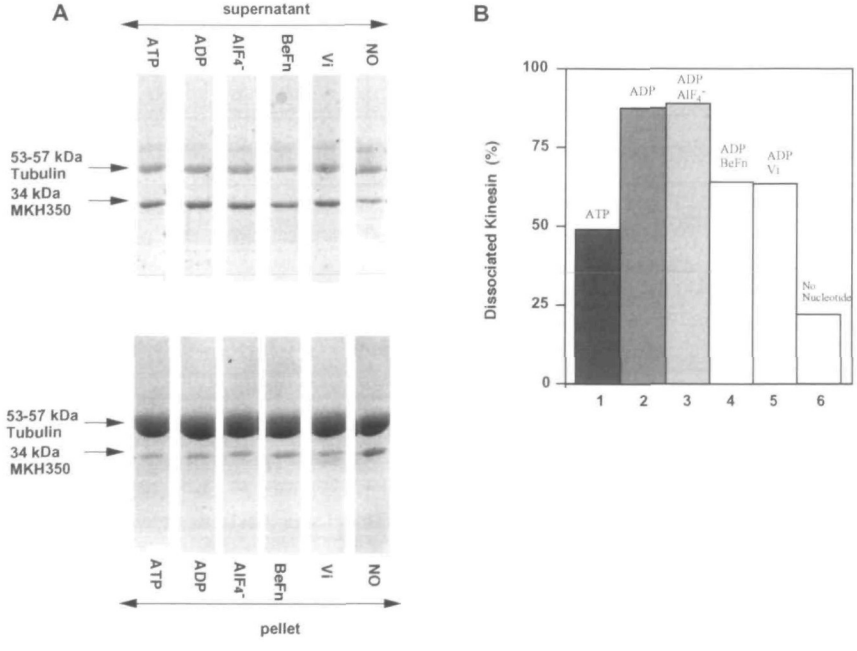

Fig. 8. **A: Coomassie Blue-stained SDS gels of microtubule (MT) pelleting assays.** To 4 μM of MKH350 in the presence of 1 mM ATP, 1 mM ADP, no nucleotide or 1 mM ADP + 1 mM P_i analogues, 6 μM MTs was added. After centrifugation, the supernatant and pellet were subjected to SDS-PAGE. **B: Rate of dissociated MKH350 from MT·MKH350.** Dissociation constants (%) = (The concentration of MKH350 in supernatant in the absence or presence of nucleotide and ADP·P_i analogues)/(The concentration of MKH350 in supernatant in the absence of nucleotide and MT) × 100. Band intensities were analyzed with an Image analyzer.

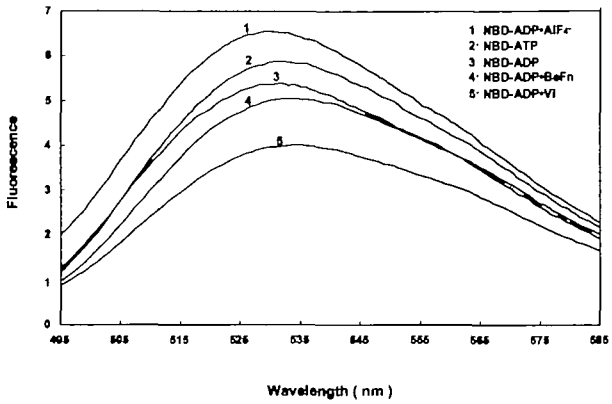

Fig. 9. **Fluorescence emission spectrum of MKH350·NBD-ADP·P_i analogues ternary complexes.** (1) 1 mM AlF_4^- + 0.3 μM NBD-ADP in buffer A (1.5 μM MKH350, 120 mM NaCl, 30 mM Tris-HCl, pH 7.5, and 2 mM $MgCl_2$). (2) 0.3 μM NBD-ATP in buffer A. (3) 0.3 μM NBD-ADP in buffer A. (4) 1 mM BeF_n + 0.3 μM NBD-ADP in buffer A. (5) 1 mM V_i + 0.3 μM NBD-ADP in buffer A. The excitation was at 475 nm.

these conditions in the absence of nucleotide, 80% MKH350 was found in pellet with microtubules. In the presence of nucleotides, 87% and 50% of MKH350 for ADP and ATP, respectively was found in the supernatant free of microtubules. These results are consistent with previous reports suggesting that kinesin dissociates from microtubules in the kinesin·ADP state but not the kinesin·ATP state. In the presence of ADP and AlF_4^-, 90% of MKH350 was in the supernatant, suggesting that the MKH350·ADP·AlF_4^- complex is in a similar state to MKH350·ADP. In the presence of ADP and BeF_n or V_i, 62–63% of MKH was free of microtubules.

Fluorescence Spectra of Kinesin·NBD-ADP·Fluorometal Ternary Complexes—Fluorescence spectra of MKH350·NBD-ADP·AlF_4^-, BeF_n or V_i complexes were measured (Fig. 9). Fluorescence emission maximum of the MKH350·NBD-ADP·AlF_4^- was 530 nm, which was identical to that of MKH·ADP. In contrast, the fluorescence maximum of the MKH350·NBD-ADP·AlF_4^- and MKH350·NBD-ADP·V_i complexes showed a slight red-shift at 533 nm as seen in the presence of NBD-ATP. Although differences in the spectra were not significant, the results demonstrated that the MKH350·NBD-ADP·AlF_4^- complex has a slightly different environment around the bound nucleotide from the other complexes, but a similar kinesin·ADP.

DISCUSSION

To determine the molecular mechanism by which ATP chemical energy is transmitted to the mechanical motility energy of kinesin, we investigated the sequential conformational change of the kinesin motor domain during ATP hydrolysis that may be directly related to energy transduction. Previous kinetic studies demonstrated that during ATP hydrolysis, kinesin forms a series of intermediates (*25, 30–32*). In this study, we used fluorometals (AlF_4^-, BeF_n) as known phosphate analogues to form stable kinesin·ADP·fluorometal ternary complexes, which may mimic the transient intermediate complexes in the kinesin ATPase cycle. We have previously demonstrated that, in the presence of Mg-ADP, myosin forms stable ternary complexes with fluorometals, and the complexes mimic the transient intermediates in the ATPase kinetic pathway (*12, 16, 18*). Recent crystallographic studies have shown that the structures of the motor domains of myosin and kinesin are highly conserved (*2–4, 33*). Thus, these motor proteins may share common mechanisms for generating energy for motility from ATP hydrolysis. Therefore, we reasoned that, as for myosin, kinesin·ADP·fluorometals ternary complexes should be formed which mimic intermediates in the kinesin ATPase cycle. Actually, the formation of kinesin·ADP·AlF_4^-, kinesin·ADP·BeF_n, and kinesin·ADP·V_i was monitored using fluorescence and the ADP analogue NBD-ADP (Fig. 4). Indeed, it is of interest to compare the properties of kinesin·ADP·fluorometal ternary complexes with myosin·ADP·fluorometal ternary complexes. We found that the kinesin complexes were much less stable than the complexes of myosin·ADP·fluorometals, which have lifetimes of several days. The unusual stabilities for myosin·ADP·fluorometals ternary complexes may be due to the presence of several unique loops in myosin at the entrance of the ATP-binding cleft, which have not been observed in kinesin (*4*). The more rapid formation of kinesin·ADP·AlF_4^- complexes (Table I) may also be explained by the lack of these extra loops. Actually, we have demonstrated that conformation of one of the unique loops of myosin, loop M containing Lys 681, changes during the ATPase cycle, suggesting that the loop acts as a signal transducer mediating communication between the ATP- and actin-binding sites (*34, 35*). Moreover, the point mutation at the unique loop L5 of kinesin significantly changes ATPase activity (our unpublished data).

The fluorescent properties of NBD-ATP for kinesin were significantly different than those for myosin. As shown in Fig. 4, when NBD-ATP bound to kinesin, the fluorescence intensity was increased by 3-fold. In contrast, NBD-ATP bound to myosin showed a 40% decrease of fluorescence intensity. These results suggest that the NBD fluorophore, which is known to be highly environmentally sensitive (*36*), reflects the precise conformational differences around the ATP-binding cleft between kinesin and myosin, even though the structures of the motor domains of myosin and kinesin are highly conserved. The differences may affect the formation and stability of the ternary complexes.

The microtubule-kinesin mechanism shows a different pathway from that of actomyosin. Gilbert *et al.* (*37*) demonstrated that dissociation of the kinesin occurred after the hydrolysis step, while dissociation occurs before hydrolysis for actomyosin. Therefore, it is of interest to determine the steps in the microtubule-kinesin ATPase cycle that mimic the kinesin·ADP·fluorometals ternary complex. We have previously demonstrated that the myosin·ADP·AlF_4^- and myosin·ADP·BeF_n complexes mimic, respectively, the M^{**}·ADP·P_i and M^*·ATP states, in which myosin dissociates from actin (*12*). As shown in Fig. 8B, the interaction of kinesin·ADP·fluorometal complexes with microtubules suggests that the kinesin·ADP·AlF_4^- complex may mimic the kinesin·ADP state, in which kinesin dissociates. In contrast, kinesin·ADP·BeF_n may mimic the kinesin·ADP·P_i state, in which kinesin associates with microtubules. This is also suggested by the fluorescent emission maximum (530 nm) of the kinesin·ADP·AlF_4^-, which is identical in value to that of kinesin in the presence of NBD-ADP, which was apparently blue-shifted from that of kinesin·NBD-

ADP·BeF_n and kinesin in the presence of NBD-ATP. Interestingly, the ternary complex using vanadate, which is also known as a phosphate analogue, mimics the kinesin·ADP·P_i state, similar to the BeF_n complex (*38*). Although these two phosphate analogues form distinct complexes, they each mimic a different state in the myosin ATPase cycle. The formation of the kinesin·ADP·AlF_4^- complex was confirmed by chasing with an excess of ATP the NBD-ADP from the ternary complex (Figs. 5 and 6), indicating a slow release rate constant.

In conclusion, we demonstrated in the present study that kinesin formed ternary complexes (kinesin·ADP·fluorometals) with new phosphate analogues of fluorometals in the presence of Mg-ADP. The fluorescence spectra and interactions of the ternary complexes with microtubules suggest that the ternary complexes mimic the transient state in the kinesin ATPase kinetic pathway. Thus, kinesin·ADP·AlF_4^- and kinesin·ADP·BeF_n complexes correspond to the kinesin·ADP and kinesin·ADP·P_i states, respectively. Finally, our data suggest that the kinesin·ADP·fluorometal ternary complexes may be useful for studying the molecular mechanism of energy transduction for kinesin.

REFERENCES

1. Kull, F.J., Val, R.D., and Fletterick, R.J. (1998) The case for a common ancestor: kinesin and myosin motor proteins and G proteins. *J. Muscle Res. Cell Motil.* **19**, 877–886
2. Kozielski, F., Sack, S., Marx, A., Thormahlen, M., Schonbrunn, E., Biou, V., Thompson, A., Mandelkow, E.M., and Mandelkow, E. (1997) The crystal structure of dimeric kinesin and implications for microtubule-dependent motility. *Cell* **91**, 985–994
3. Sack, S., Muller, J., Marx, A., Thormahlen, M., Mandelkow, E.M., Brady, S.T., and Mandelkow, E. (1997) X-ray structure of motor and neck domains from rat brain kinesin. *Biochemistry* **36**, 16155–16165
4. Kull, F.J., Sablin, E.P., Lau, R., Fletterick, R.J., Vale, R.D. (1996) Crystal structure of the kinesin motor domain reveals a structural similarity to myosin. *Nature* **380**, 550–555
5. Vale, R.D. (1996) Switches, latches, and amplifiers: common themes of G proteins and molecular motors. *J. Cell Biol.* **135**, 291–302
6. Furch, M., Fujita-Becker, S., Geeves, M.A., Holmes, K.C., and Manstein, D.J. (1999) Role of the salt-bridge between switch-1 and switch-2 of *Dictyostelium* myosin. *J. Mol. Biol.* **290**, 797–809
7. Howard, J., Hudspeth, A.J., and Vale, R.D. (1989) Movement of microtubules by single kinesin molecules. *Nature* **342**, 154–158
8. Block, S.M., Goldstein, L.S., and Schnapp, B.J. (1990) Bead movement by single kinesin molecules studied with optical tweezers. *Nature* **348**, 348–352
9. Finer, J.T., Simmons, R.M., and Spudich, J.A. (1994) Single myosin molecule mechanics: piconewton forces and nanometre steps. *Nature* **368**, 98–99
10. Ishijima, A., Harada, Y., Kojima, H., Funatsu, T., Higuchi, H., and Yanagida, T. (1994) Single-molecule analysis of the actomyosin motor using nano-manipulation. *Biochem. Biophys. Res. Commun.* **199**, 1057–1063
11. Romberg, L. and Vale, R.D. (1993) Chemomechanical cycle of kinesin differs from that of myosin. *Nature* **361**, 168–170
12. Maruta, S., Henry, G.D., Sykes, B.D., and Ikebe, M. (1993) Formation of the stable myosin-ADP-aluminum fluoride and myosin-ADP-beryllium fluoride complex and their analysis using ^{19}F-NMR. *J. Biol. Chem.* **268**, 7093–7100
13. Werber, M.M., Peyser, Y.M., and Muhlrad, A. (1992) Characterization of stable beryllium fluoride, aluminum fluoride, and vanadate containing myosin subfragment 1-nucleotide complexes. *Biochemistry* **31**, 7190–7197
14. Phan, B. and Reisler, E. (1992) Inhibition of myosin ATPase by beryllium fluoride. *Biochemistry* **31**, 4787–4793
15. Gopal, D. and Burke, M. (1995) Formation of stable inhibitory complexes of myosin subfragment 1 using fluoroscandium anions. *J. Biol. Chem.* **270**, 19282–19286
16. Maruta, S., Uyehara, Y., Homma, K., Sugimoto, Y., and Wakabayashi, K. (1999) Formation of the myosin·ADP·gallium fluoride complex and its solution structure by small-angle synchrotron X-ray scattering. *J. Biochem.* **125**, 177–185
17. Park, S., Ajtai, K., and Burghardt, T.P. (1999) Inhibition of myosin ATPase by metal fluoride complexes. *Biochim. Biophys. Acta* **1430**, 127–140
18. Maruta, S., Aihara, T., Uyehara, Y., Homma, K., Sugimoto, Y., and Wakabayashi, K. (2000) Solution structure of myosin-ADP-MgF_n ternary complex by fluorescent probes and small-angle synchrotron X-ray scattering. *J. Biochem.* **128**, 687–694
19. Fisher, A.J., Smith, C.A., Thoden, J.B., Smith, R., Sutoh, K., Holden, H.M., and Rayment, I. (1995) X-ray structures of the myosin motor domain of *Dictyostelium discoideum* complexed with MgADP·BeF_x and MgADP·AlF_4^-. *Biochemistry* **34**, 8960–8972
20. Smith, C.A. and Rayment, I. (1996) X-ray structure of the magnesium(II)·ADP·vanadate complex of the *Dictyostelium discoideum* myosin motor domain to 1.9 Å resolution. *Biochemistry* **35**, 5404–5417
21. Antonny, B. and Chabre, M. (1992) Characterization of the aluminum and beryllium fluoride species which activate transducin. Analysis of the binding and dissociation kinetics. *J. Biol. Chem.* **267**, 6710–6718
22. Bigay, J., Deterre, P., Pfister, C., and Chabre, M. (1985) Fluoroaluminates activate transducin-GDP by mimicking the gamma-phosphate of GTP in its binding site. *FEBS. Lett.* **191**, 181–185
23. Bigay, J., Deterre, P., Pfister, C., and Chabre, M. (1987) Fluoride complexes of aluminium or beryllium act on G-proteins as reversibly bound analogues of the gamma phosphate of GTP. *EMBO J.* **6**, 2907–2913
24. Sondek, J., Lambright, D.G., Noel, J.P., Hamm, H.E., and Sigler, P.B. (1994) Protein, structure GTPase mechanism of G proteins from the 1.7-Å crystal structure of transducin alpha-GDP-AIF-4. *Nature* **372**, 276–279
25. Hackney, D.D. (1988) Kinesin ATPase: Rate-limiting ADP release. *Proc. Natl. Acad. Sci. USA* **85**, 6314–6318
26. Laemmli, U.K. (1970) Cleavage of structural proteins during the assembly of the head of bacteriophage T4. *Nature* **227**, 680–685
27. Maruta, S., Mizukura, Y., and Chaen, S. (2002) Interaction of a new fluorescent ATP analogue with skeletal muscle myosin subfragment-1. *J. Biochem.* **131**, 905–911
28. Guillory, R.J. and Jeng, S.J. (1977) Arylazido nucleotide analogs in a photoaffinity approach to receptor site labeling. *Methods Enzymol.* **46**, 259–288
29. Lockhart, A., Crevel, I.M., Cross, R.A. (1995) Kinesin and ncd bind through a single head to microtubules and compete for a shared MT binding site. *J. Mol. Biol.* **249**, 763–771
30. Ma, Y.Z. and Taylor, E.W. (1997) Kinetic mechanism of a monomeric kinesin construct. *J. Biol. Chem.* **272**, 717–723
31. Sadhu, A. and Taylor, E.W. (1992) A kinetic study of the kinesin ATPase. *J. Biol. Chem.* **267**, 11352–11359
32. Ma, Y.Z. and Taylor, E.W. (1995) Kinetic mechanism of kinesin motor domain. *Biochemistry* **34**, 13233–13241
33. Rayment, I., Rypniewski, W.R., Schmidt-Base, K., Smith, R., Tomchick, D.R., Benning, M.M., Winkelmann, D.A., Wesenberg, G., and Holden, H.M. (1993) Three-dimensional structure of myosin subfragment-1: a molecular motor. *Science* **261**, 35–36
34. Maruta, S. and Homma, K. (1998) A unique loop contributing to the structure of the ATP-binding cleft of skeletal muscle myosin communicates with the actin-binding site. *J. Biochem.* **124**, 528–533
35. Maruta, S. and Homma, K. (2000) Conformational changes in the unique loops bordering the ATP binding cleft of skeletal muscle myosin mediate energy transduction. *J. Biochem.* **128**, 695–704
36. Chattopadhyay, A. (1990) Chemistry and biology of *N*-(7-nitrobenz-2-oxa-1,3-diazol-4-yl)-labeled lipids: fluorescent probes of biological and model membranes. *Chem. Phys. Lipids* **53**, 1–15
37. Gilbert, S.P., Webb, M.R., Brune, M., and Johnson, K.A. (1995) Pathway of processive ATP hydrolysis by kinesin. *Nature* **373**, 671–676
38. Goodno, C.C. (1979) Inhibition of myosin ATPase by vanadate ion. *Proc. Natl. Acad. Sci. USA* **76**, 2620–2624